

RESEARCH

Open Access



Pan-tumor survey of *ROS1* fusions detected by next-generation RNA and whole transcriptome sequencing

Misako Nagasaka^{1,2,3*}, Shannon S. Zhang¹, Yasmine Baca⁴, Joanne Xiu⁴, Jorge Nieva⁵, Ari Vanderwalde⁴, Jeffrey J. Swensen⁴, David Spetzler⁴, Wolfgang Michael Korn⁶, Luis E. Raez⁷, Stephen V. Liu⁸ and Sai-Hong Ignatius Ou^{1,2}

Abstract

Background Two *ROS1* tyrosine kinase inhibitors have been approved for *ROS1* fusion positive (*ROS1*+) non-small cell lung cancer (NSCLC) tumors. We performed a pan-tumor analysis of the incidence of *ROS1* fusions to assess if more *ROS1*+ patients who could benefit from *ROS1* TKIs could be identified.

Methods A retrospective analysis of *ROS1* positive solid malignancies identified by targeted RNA sequencing and whole transcriptome sequencing of clinical tumor samples performed at Caris Life Science (Phoenix, AZ).

Results A total of 259 *ROS1*+ solid malignancies were identified from approximately 175,350 tumors that underwent next-generation sequencing (12% from targeted RNA sequencing [Archer]; 88% from whole transcriptome sequencing). *ROS1*+ NSCLC constituted 78.8% of the *ROS1*+ solid malignancies, followed by glioblastoma (GBM) (6.9%), and breast cancer (2.7%). The frequency of *ROS1* fusion was approximately 0.47% among NSCLC, 0.29% for GBM, 0.04% of breast cancer. The mean tumor mutation burden for all *ROS1*+ tumors was 4.8 mutations/megabase. The distribution of PD-L1 (22C3) expression among all *ROS1*+ malignancies were 0% (18.6%), 1–49% (29.4%), and $\geq 50\%$ (60.3%) [for NSCLC: 0% (17.8%); 1–49% (27.7%); $\geq 50\%$ (53.9%).

The most common genetic co-alterations of *ROS1*+ NSCLC were *TP53* (29.1%), *SETD2* (7.3%), *ARIAD1A* (6.3%), and *U2AF1* (5.6%).

Conclusions *ROS1*+ NSCLC tumors constituted the majority of *ROS1*+ solid malignancies with four major fusion partners. Given that $> 20\%$ of *ROS1*+ solid tumors may benefit from *ROS1* TKIs treatment, comprehensive genomic profiling should be performed on all solid tumors.

Keywords c-*ROS1*, Receptor tyrosine kinase fusions, Non-small cell lung cancer, Breast cancer, Pan-tumor analysis

*Correspondence:

Misako Nagasaka
nagasakm@hs.uci.edu

Full list of author information is available at the end of the article



© The Author(s) 2023. **Open Access** This article is licensed under a Creative Commons Attribution 4.0 International License, which permits use, sharing, adaptation, distribution and reproduction in any medium or format, as long as you give appropriate credit to the original author(s) and the source, provide a link to the Creative Commons licence, and indicate if changes were made. The images or other third party material in this article are included in the article's Creative Commons licence, unless indicated otherwise in a credit line to the material. If material is not included in the article's Creative Commons licence and your intended use is not permitted by statutory regulation or exceeds the permitted use, you will need to obtain permission directly from the copyright holder. To view a copy of this licence, visit <http://creativecommons.org/licenses/by/4.0/>. The Creative Commons Public Domain Dedication waiver (<http://creativecommons.org/publicdomain/zero/1.0/>) applies to the data made available in this article, unless otherwise stated in a credit line to the data.

Background

Receptor tyrosine kinase (RTK) fusion has been recognized as oncogenic structural gene rearrangements in solid malignancies [1]. Among the 58 human RTKs [2], there are US Food and Drug Administration (FDA) approved treatments in anaplastic lymphoma kinase (*ALK*), c-ROS1 (*ROS1*), rearranged in transformation (*RET*), fibroblastic growth factor receptor (*FGFR2-3*), and neutrophin receptor tyrosine kinase (*NTRK1-3*) fusion positive tumors. With the exception of *NTRK* and *RET* fusions, all of the US FDA approvals are tumor-specific: *ALK* (non-small cell lung cancer [NSCLC]), *ROS1* (NSCLC), and *FGFR2-3* (urothelial, cholangiocarcinoma). Although these RTK fusions are found in all solid tumors albeit in a lower frequency, the main biology of the pathological process is universal and not tumor histology-specific. Therefore, it is important to identify RTK fusions systematically beyond the specific tumor histologic types with approved treatments to expand the horizon of RTK fusion patients who may benefit from the expanded approval of treatments by raising awareness among clinicians, pharmaceutical companies and regulatory authorities to screen and enroll these patients in future clinical trials.

In this study, we performed a large-scale pan-tumor survey of *ROS1* fusions detected by next generation RNA sequencing to identify and characterize the molecular characteristics of *ROS1*+ solid tumors.

Methods

Patient cohort

A total of 259 *ROS1*+ tumors were identified in a retrospective assessment of a deidentified molecular profiling database surveyed for solid tumors that underwent fusion testing from a cohort including all cases submitted to a Clinical Laboratory Improvement Amendments (CLIA)–certified laboratory (Caris Life Sciences, Phoenix Arizona) for comprehensive genomic profiling. All unique cases that underwent successful fusion testing for targeted RNA sequencing were identified and included in this study.

This study was conducted in accordance with guidelines of the Declaration of Helsinki, Belmont report, and U.S. Common rule. In keeping with 45 CFR 46.101 (b) [4], this study was performed utilizing retrospective, deidentified clinical data. The need for written informed consent and ethical approval was waived by the University of California Irvine ethic committee due to the retrospective nature of the study. Table 1 shows the list of cancer type studied in this cohort.

Table 1 List of cancer types in studied cohort

Cancer Type	N
Non-small cell lung cancer (NSCLC)	204
High Grade Glioma	18
Breast Carcinoma	7
Pancreatic Adenocarcinoma	4
Ovarian	4
Cancer of Unknown Primary	3
Cholangiocarcinoma	3
Colorectal Adenocarcinoma	3
Gastric Adenocarcinoma	3
Sarcoma	3
Esophageal and Esophagogastric Junction Carcinoma	2
Bladder cancer—urothelial	1
Melanoma	1
Neuroendocrine tumors	1
Small Intestinal Malignancies	1
Thyroid Carcinoma	1
Total	259

Fusion detection

Detailed methods on targeted RNA sequencing and whole transcriptome sequencing (WTS) have been previously described [3]. For tumors tested before February 2019, targeted RNA next generation-sequencing (NGS) was performed. For tumors tested after February of 2019, gene fusion detection was performed as part of whole transcriptome sequence (WTS) analysis on mRNA isolated from a formalin-fixed paraffin-embedded tumor sample using the Illumina NovaSeq platform (Illumina, Inc., San Diego, CA) and Agilent SureSelect Human All Exon V7 bait panel (Agilent Technologies, Santa Clara, CA). FFPE specimens underwent pathology review to diagnose percent tumor content and tumor size; a minimum of 10% of tumor content in the area for microdissection was required to enable enrichment and extraction of tumor-specific RNA. Qiagen RNA FFPE tissue extraction kit was used for extraction, and the RNA quality and quantity was determined using the Agilent TapeStation.

For tumors tested prior to February of 2019, anchored multiplex PCR was performed for targeted RNA NGS using the ArcherDx fusion assay (Archer FusionPlex Solid Tumor panel). The formalin-fixed paraffin-embedded tumor samples were microdissected to enrich the samples to $\geq 20\%$ tumor nuclei, and mRNA was isolated and reverse transcribed into complementary DNA (cDNA). Unidirectional gene-specific primers were used to enrich for target regions, followed by NGS (Illumina MiSeq platform). Targets included 52 genes, and the full list can be found at <http://archerdx.com/fusio>

nplex-assays/solid-tumor. In the studied cohort, 55 samples were tested using ArcherDx fusion assay and 204 were testing using WTS.

PD-L1 expression (TPS score)

NSCLC tumors tested after January of 2016 were stained with PD-L1 using primary PD-L1 antibody clone of 22c3 (Dako). Tumor Proportion Score (TPS) was measured, which is the percentage of viable tumor cells showing partial or complete membrane staining at any intensity. The tumor was considered positive if $TPS \geq 1\%$ (high PD-L1 expression if $TPS \geq 50\%$).

Tumor mutation burden (TMB)

TMB was measured (592 genes and 1.4 megabases [MB] sequenced per tumor) by counting all non-synonymous missense mutations found per tumor that had not been previously described as germline alterations according to dbSNP and 1 KG databases.

TMB was adjusted by dividing by a factor of 1.2 and a cutoff point of ≥ 10 mutations per MB was used based on the KEYNOTE-158 pembrolizumab trial [4], which showed that patients who had failed standard of care therapy and a TMB of ≥ 10 mt/MB across several tumor types had higher response rates than patients with a TMB of < 10 mt/MB. Caris Life Sciences is a participant in the Friends of Cancer Research TMB Harmonization Project [5].

Survival and statistical analysis

Survival analysis was performed using real-world evidence from insurance claims data and calculated from time of tissue collection to last contact or time on treatment using Kaplan–Meier survival analysis. JMP statistical software was used to calculate mean/median tumor mutation burden (TMB), standard deviation (SD) and range as well as the mean junction read. Statistical significance was determined using chi-square and Wilcoxon rank sum test and adjusted for multiple comparisons.

Results

Incidence and distribution of *ROS1*+ solid tumors

A total of 259 *ROS1* fusions in solid tumors were detected by NGS RNA from 175,350 unique tumor samples composed of 16 different tumor types. Among these 175,350 tumor samples, 154,200 samples were profiled by WTS and 21,150 were profiled by NGS targeted RNA sequencing (Archer). Thus, the overall incidence of in-frame *ROS1*+solid tumors was 0.15% (259/175350) by RNA NGS. The clinical characteristics of the three most common tumor type with *ROS1* fusions is summarized in Table 2.

ROS1+NSCLC tumors made up of 78.8% of the *ROS1*+solid tumors, followed by *ROS1*+GBM (6.9%), and *ROS1*+breast cancer (2.7%) followed by 1–3 cases of *ROS1* fusions among the the rest of the 13 tumor types (Fig. 1A body figure, Fig. 1B pie chart). A total of 33 different fusion partners were identified among the *ROS1*+solid tumors (Fig. 1C, Supplementary Table 1). The distribution of the fusions partners among the *ROS1*+solid tumors are shown in Fig. 1C. The distribution of the exon breakpoints among the *ROS1*+solid tumors are shown in Fig. 1D and A comparison of overall with NSCLC and GBM are shown in Fig. 1E. The chromosomal breakpoints of *ROS1*+solid tumors are shown in Fig. 1F.

ROS1+ NSCLC tumors

Among the 259 *ROS1*+tumors, 204 (78.8%) were *ROS1*+NSCLC (Fig. 1B). The overall incidence of *ROS1*+NSCLC was approximately 0.47% (204/43404) in the database. There was no difference in the detection rates of *ROS1*+NSCLC by ArcherDx fusion assay (0.52%, 49/9393) and WTS (0.55%, =155/28173). Four fusions partners essentially made up the bulk of the *ROS1*+NSCLC with *CD74-ROS1* (34.8%) being the most common fusion variant followed by *EZR-ROS1* (25.3%),

Table 2 Patient and clinical characteristics of *ROS1*+ solid tumors

	All	NSCLC	Glioblastoma	Breast	Other
N (%)	259	204 (79%)	18 (7%)	7 (3%)	30 (11%)
Age median (range)	63 (18–89)	65 (27–89)	63 (41–89)	60 (40–77)	52.5 (18–80)
Male	113 (44%)	86 (42%)	11 (61%)	0 (0%)	16 (53%)
Female	146 (56%)	118 (58%)	7 (39%)	7 (100%)	14 (47%)
Sequencing methods					
Targeted RNA Archer (prior to 2019)	55 (21%)	49 (24%)	4 (22%)	1 (14%)	1 (3%)
WTS (post 2019)	204 (79%)	155 (76%)	14 (78%)	6 (86%)	29 (96%)
Mean junction read (SD)	54.7	64 (107.8)	32.2 (55.1)	6.7 (5.2)	25.6 (25.8)
Median TMB	4	4	3	5	4

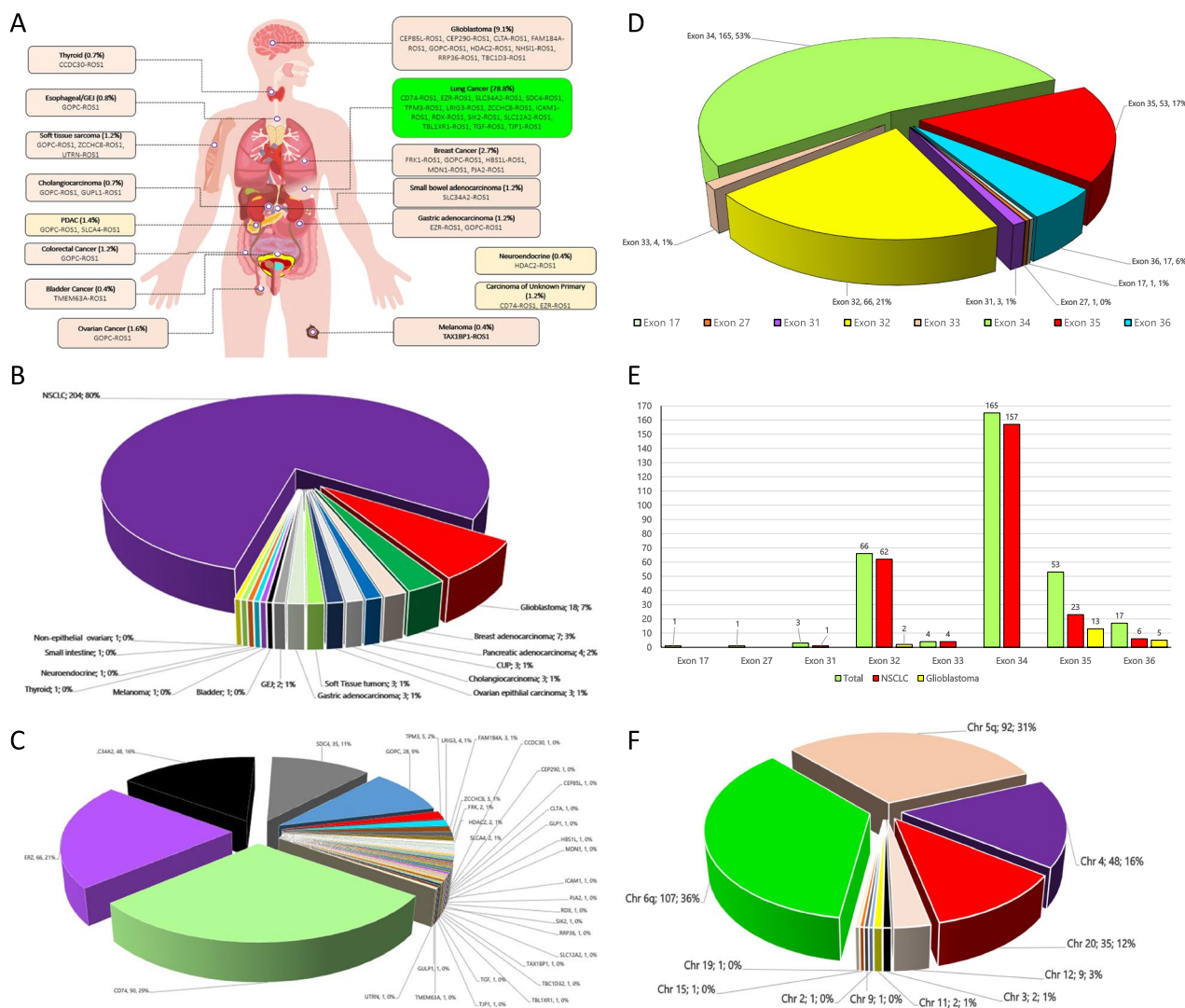


Fig. 1 **A** Schematic diagram of the primary tumor site of *ROS1* fusions and the *ROS1* fusion variants identified in tumor site. **B** Pie-chart showing the distribution of the primary site of *ROS1* fusion positive tumors. **C** Pie-chart showing the distribution of fusion partners in all *ROS1*+ solid tumors. **D** Pie chart showing the frequency of fusion breakpoint by *ROS1* exons. **E** Comparison of *ROS1* exon fusion breakpoints overall and with NSCLC and glioblastoma. **F** Pie chart showing *ROS1*+ solid tumor chromosomal breakpoints

SLC34A2-ROS1 (18.6%), and *SDC4-ROS1* (13.8%) (Fig. 2A).

The vast majority of exon breakpoints at *ROS1* spanned 4 exons (exons 32, 34, 35, 36) with exon 34 (62.1%) being the most common breakpoint (Fig. 1D). There seemed to be a correlation between exon breakpoints and the fusion partners. *CD74-ROS1* and *EZR-ROS1* fusions were more commonly generated from breakpoint at *ROS1* exon 34 (Fig. 2B and C) while *SLC34A2-ROS1* and *SDC4-ROS1* fusions were generated more commonly with *ROS1* exon 32 (Fig. 2D and E). Interestingly, the much rarer *LRIG3-ROS1* and *TPM3-ROS1* fusion variants were generated from breakpoint at *ROS1* exon 35 (Supplementary Table 2). Importantly, the

ROS1 fusion breakpoint at exon 35 or 36 both encode the transmembrane region of the *ROS1* protein. The transmembrane domain of *ROS1* protein spans amino acids 1862–1883 and the cytoplasmic domain which contain the kinase domain is between amino acids 1945–2222 with the ATP binding site within 1951–1980. (<https://www.ebi.ac.uk/interpro/protein/reviewed/P08922/>) accessed October 25, 2020).

Molecularly, the exon fusion breakpoints in exons 32, 34–36 with fusion at exon 34 was the most common especially among *ROS1*+ NSCLC tumors while exon 35 were found as fusion breakpoints for *ROS1*+ non-NSCLC tumors (Fig. 1E). Among the junctional reads

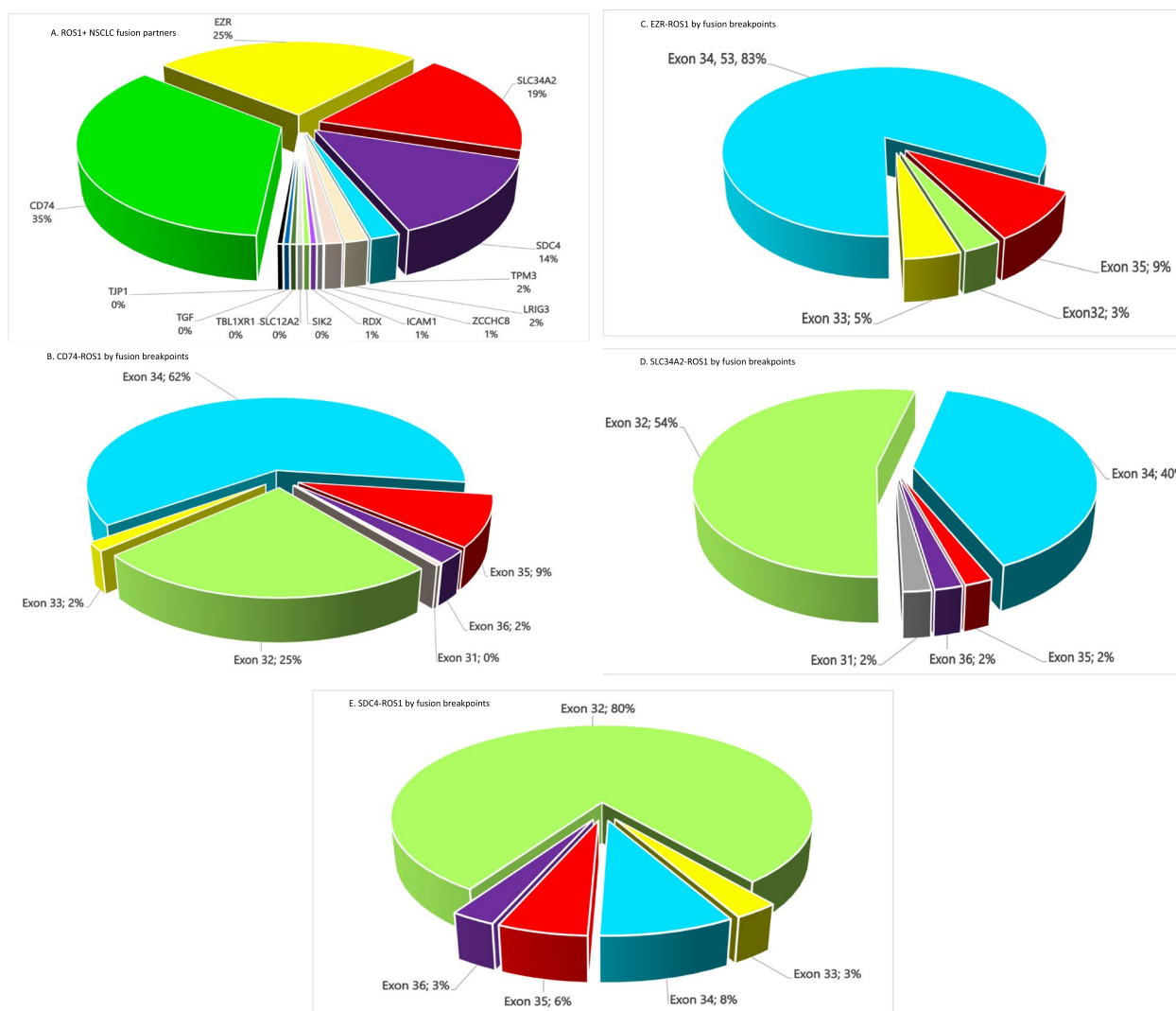


Fig. 2 **A** Pie chart showing the distribution of fusions partners in *ROS1*+NSCLC. **B** Pie chart showing the frequency of fusion breakpoint by *ROS1* exons in *CD74-ROS1*+. **C** Pie chart showing the frequency of fusion breakpoint by *ROS1* exons in *EZR-ROS1*+. **D** Pie chart showing the frequency of fusion breakpoint by *ROS1* exons in *SLC34A2-ROS1*+. **E** Pie chart showing the frequency of fusion breakpoint by *ROS1* exons in *SDC4-ROS1*+

of the major *ROS1*+tumors, the highest was among NSCLC, followed by GBM. Of note, *ROS1*+breast adenocarcinoma, though with limited number of samples, had a tenfold lower junction reads than those of *ROS1*+NSCLC (Supplementary Table 3).

In terms of biomarkers for potential efficacy for immune checkpoint inhibitors. The median tumor mutation burden (TMB) for *ROS1*+NSCLC was 4, the mean was 4.8 (SD 2.8, range 0–15) and only 4.6% of *ROS1*+NSCLC tumors had TMB ≥ 10. The percentage of tumor samples with PD-L1 expression ≥ 50% was 54.5% and ≥ 1% was 81.2% (Supplementary Fig. 1).

ROS1+ GBM

Glioblastoma was the second most common *ROS1*+fusion tumors with an incidence of 6.9% (18/259) in this pan-tumor survey. The incidence of *ROS1*+GBM was approximately 0.29% (18/6206). GOPC was the most common fusion partner (50%) (Fig. 3A). Figure 3B shows the frequency of fusion breakpoint by *ROS1* exons in *ROS1*+GBM.

All of the GBM samples had TMB < 10 mt/MB with a median TMB of 3 (Table 2). The majority of GBM had no PD-L1 expression (66.7%) and no samples had a PD-L1 expression ≥ 50%.

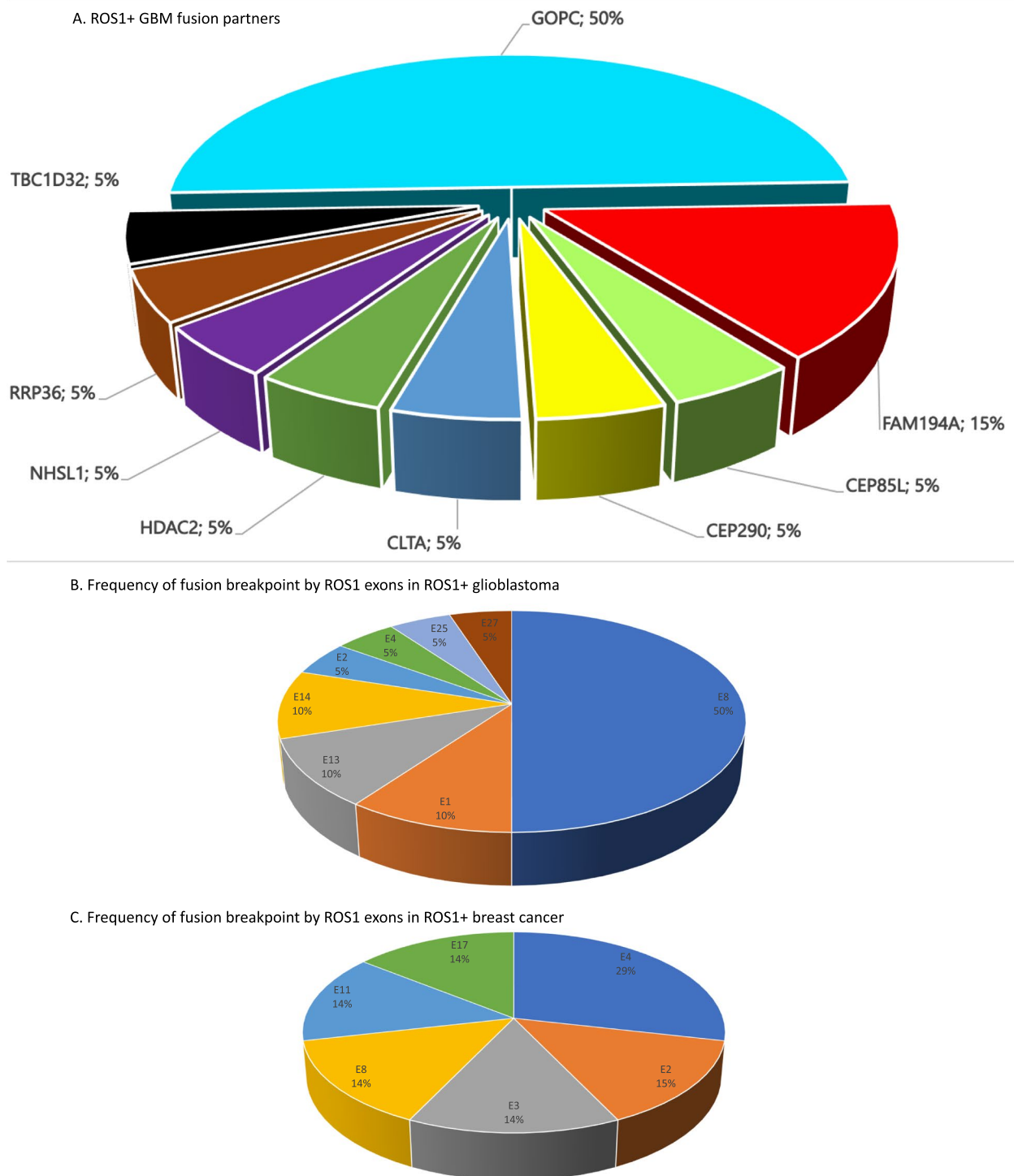


Fig. 3 **A** Pie chart showing the frequency of fusion partners in *ROS1*+ glioblastoma multiforme. **B** Pie chart showing the frequency of fusion breakpoint by *ROS1* exons in *ROS1*+ glioblastoma multiforme. **C** Pie chart showing the frequency of fusion breakpoint by *ROS1* exons in *ROS1*+ breast cancers

ROS1+ breast cancer tumors

ROS1+ breast cancer is the third most common ROS1 fusion constituting 2.7% of the ROS1+ solid tumors (Fig. 1B). The incidence of ROS1+ breast cancer in the database was approximately 0.04% (7/17500). The hormonal status of the five ROS1+ breast cancer cases are listed in Table 3. One of the GPOC-ROS1 had a unique exon breakpoint at exon 17 of ROS1 (Fig. 3C).

Mean allele (fusion) frequency

The mean number of junctional read among all tumor types was 54.7 with NSCLC at 64.0 (SD 107.77), glioblastoma at 32.2 (SD 55.12) and breast cancer at 6.7 (SD 5.20) (Table 2).

Co-occurrence with other genetic aberrations

ROS1+ NSCLC were mutually exclusive with known actionable oncogenic alterations in EGFR, KRAS, ALK, RET, NTRK or NRG. TP53 mutations (29.1%) were the most common co-mutations followed by SETD2 mutations (7.3%), ARIADIA mutations (6.3%) and U2AF1 (5.6%). The complete list of genetic co-alterations are listed in (Supplementary Table 4).

PD-L1 expression

The PD-L1 expression status were determined in 191 out of the 204 ROS1+ NSCLC samples. When the 191 ROS1+ NSCLC samples with known PD-L1 status were analyzed, the distribution by PD-L1 expression were: 0% ($n=34$), 1–49% (53), and >50% (104) (Supplementary Table 5). When the 204 ROS1+ tumor samples with known PD-L1 status were analyzed, the distribution by PD-L1 expression were: 0% ($n=38$), 1–49% ($n=60$), and >50% (106) (Supplementary Table 6) and were heavily impacted by NSCLC data. 18 patients with ROS1+ glioblastoma had PD-L1 testing by SP142 and 33.3% ($n=6/18$) were positive while 4 patients with ROS1+ breast cancer had PD-L1 testing by SP142 and 25% ($n=1/4$) were positive (data not shown).

Table 3 Hormonal receptor status of the 7 ROS1+ breast cancers

Number	ROS1 fusion	Hormonal status
1	GPOC-ROS1 (G8, R35)	ER+, PR+, HER2-
2	GPOC-ROS1 (G3, R36)	ER-, PR-, HER2- (triple negative)
3	FRK-ROS1 (F2, R34)	Unknown (not done?)
4	FRK-ROS1 (F4, R32)	ER+, PR+, HER2+
5	MDN1-ROS1 (M17, R17)	ER-, PR-, HER2- (triple negative)
6	PJA2-ROS1 (P4, R36)	ER-, PR-, HER2- (triple negative)
7	HBS1L-ROS1 (H11, R27)	ER-, PR-, HER2+

Tumor mutation burden

The median TMB was 4 mutations/MB for all ROS1+ tumors ($n=259$) while it was 4 in NSCLC, 3 in GBM and 5 in breast cancer patients with ROS1 fusions (Table 2).

Real world survival data

Kaplan-Meier curves showing time from sample collection to last contact is shown in Fig. 4A–C. There was no significant statistical difference seen in the entire cohort (Fig. 4A), NSCLC (Fig. 4B) and GBM patients (Fig. 4C) stratified by ROS1 positivity. There were only 4 ROS1+ breast cancer patients who had survival outcome information and therefore insufficient to compare with the ROS1- patients. Despite the limited number of ROS1+ glioblastoma with OS survival information ($N=9$), ROS1+ GBM patients had overall approximately 6 months (170 days) shorter OS while there was no major differences between ROS1+ NSCLC versus non-ROS1+ NSCLC.

The Kaplan-Meier curve showing time on treatment showed a non-statistical significant trend of worse outcomes with immunotherapy use versus TKI use with a median number of treatment days of 210.0 days for ROS1 positive NSCLC patients receiving TKIs (ceritinib, crizotinib, entrectinib, lorlatinib) versus median number of 70.0 days on treatment for ROS1 positive NSCLC patients receiving immunotherapy with pembrolizumab (HR = 2.766, 95% CI 0.847–9.305, $p=0.077$) although the sample size was limited (Fig. 4D).

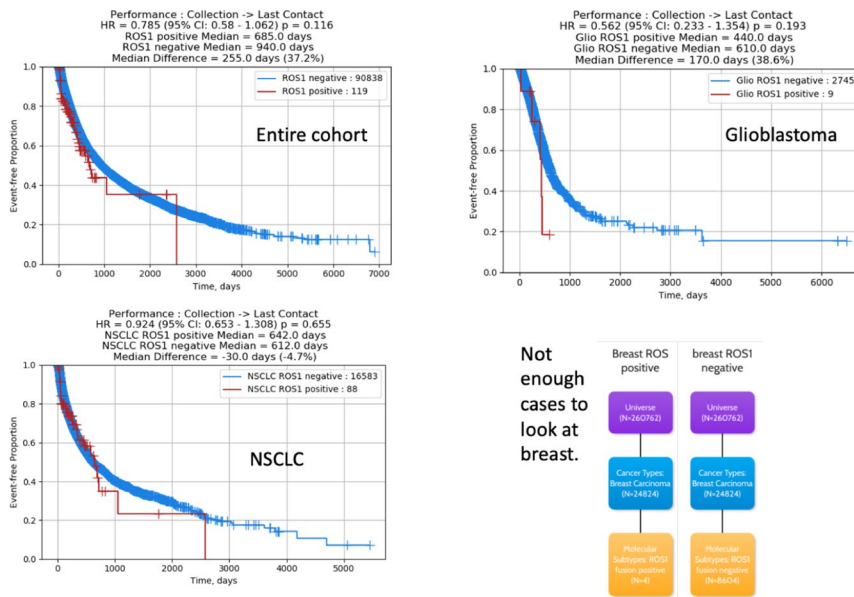
Discussion

In this first large scale survey of ROS1 fusions identified by RNA NGS where only in-frame messenger RNA (mRNA) transcripts were reported, we identified 259 ROS1+ tumor samples by RNA NGS of tumor samples spanning 16 tumor types. Many inter/intragenic rearrangements have been reported in the literature using pure DNA NGS, but whether an in-frame mRNA were eventually transcribed (and the exact ROS1 fusion variant) remained to be determined especially if clinical response was not reported [6, 7].

From the example of NTRK fusions, it is generally accepted that RTK fusions are likely an universal actionable driver among the vast majority if not all tumor types harboring that RTK fusion [1]. While ROS1+ NSCLC tumors were the dominant tumor type at 78.8% and has US FDA approved treatment of two ROS1 TKIs [8, 9], it implies that potentially more than 20% of the ROS1+ solid tumor may benefit from currently approved ROS1 TKIs.

Importantly, ROS1+ GBM constituted the second largest ROS1+ tumors at 6.9%. In fact ROS1 fusion was first identified in glioblastoma multiforme in

Kaplan Meir curves showing entire cohort (4A), NSCLC (4B) and Glioblastoma(4C)



D. ROS1 NSCLC receiving IO or TKI

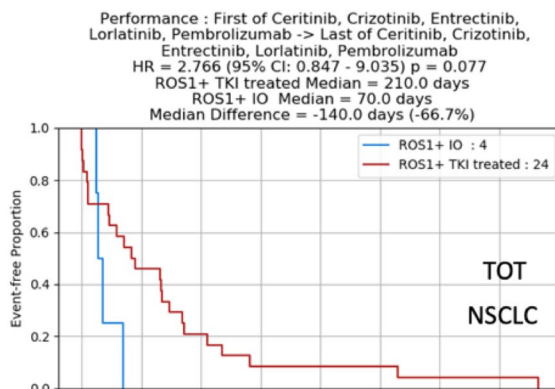


Fig. 4 A Kaplan Meir curves showing ROS1 positive vs ROS1 negative in the entire cohort. B Kaplan Meir curves showing ROS1 positive vs ROS1 negative in the NSCLC cohort. C Kaplan Meir curves showing ROS1 positive vs ROS1 negative in the glioblastoma cohort. D Kaplan Meir curves showing time on treatment of ROS1+ NSCLC patients receiving ROS1 TKIs versus immunotherapy

1987 [10]. Thus, it not surprising that ROS1+GBM constituted the second most common ROS1+ solid tumors. Although limited by the numbers of ROS1+glioblastoma identified and thus statistically not significant, the presence of ROS1 fusions in glioblastoma seems to indicate a poor prognosis. Entrectinib, a first-generation ROS1 TKI, has CNS activity and second generation ROS1 TKIs in clinical development such as repotrectinib, taletrectinib and NVL-520, also has either demonstrated CNS activity clinically or in pre-clinical models and thus could be considered as a potential treatment option for ROS1+ GBM patients [9, 11–13].

ROS1+breast adenocarcinoma was the third most common ROS1+solid tumors but only at 3%. Other ROS1 fusion positive tumors that have been previously reported in the literature such as ROS1+melanoma [14] and ROS1+ soft tissue tumor (inflammatory myofibroblastic tumor [IMT]; [15] were also identified in the database.

Molecularly, the exon fusion breakpoints in exons 32, 34–36 with fusion at exon 34 was the most common especially among ROS1+NSCLC while exon 35 were found as fusion breakpoints for ROS1+non-NSCLC tumors. Among the junctional reads of the major ROS1+ tumors, the highest was among NSCLC, followed

by GBM. Of note, *ROS1*+breast adenocarcinoma, although with limited number of samples, had a tenfold lower junction reads than those of *ROS1*+NSCLC. Additionally, two *ROS1*+breast adenocarcinoma had fusion breakpoints at exon 17 and exon 27, respectively.

In our study, *ROS1* fusions were also detected at similar frequency as previously reported *ROS1*+NSCLC tumors of approximately 2% [16] in other major tumors such as breast and pancreatic cancers. This is consistent with prior reports of identification of *ROS1* beyond NSCLC [17–24]. While the second most common tumor type glioblastoma is considered rare, the third most common tumor type in our study was breast cancer, which is one of the most common types of tumor. A previous Chinese study of 1440 breast cancer patients described a total of 30 RTK events including 3 with *ROS1* [18]. Although the hormonal status of these patients were not described in the paper, a prior case report on inflammatory breast cancer harboring *CD74-ROS1* was triple negative [17] and so were 3 out of 7 cases of *ROS1*+breast cancer in our study. Triple negative breast cancer patients are known to have less treatment options. Thus, it is important to profile tumors beyond NSCLC for *ROS1* fusions given there are now two approved tyrosine kinase inhibitors for the treatment of *ROS1*+NSCLC.

By far, the most common *ROS1*+tumor type was NSCLC. We identified 8 of the 24 *ROS1*+NSCLC fusion partners reported in the literature [25]. However, 4 (*CD74*, *EZR*, *SLC34A2* and *SDC4*) of the fusion partners made up the vast majority of the *ROS1*+NSCLC fusion partners. Neel et al. have demonstrated that different fusion partners affect the subcellular localization of the *ROS1* fusions [26] while Li et al. has described that *ROS1*+NSCLC patients with *CD74-ROS1* fusion partners are more likely to present with brain metastases and showed a trend toward improved survival in the non-*CD74-ROS1* group when they were treated with crizotinib [27], suggesting the possibility that fusion partners may have differential responses to therapy. As in the case with *ALK*-rearranged NSCLC, concurrent mutations such as *TP53* may also play a role on differential responses to targeted therapy [28] and further exploration in the space of fusion partners and concurrent mutations in *ROS1*+NSCLC is eagerly awaited.

Also notable in this brief report is the fact that to our knowledge, this is the first large scale survey of PD-L1 expression among *ROS1*+NSCLC. PD-L1 expression was detected in 81.2% of the *ROS1*+NSCLC samples where the PD-L1 expression was known. The majority of the PD-L1 positive *ROS1*+NSCLC ($\geq 1\%$) were high expressors (54.5%, 104/191). In these patients, clinicians may be tempted to use single agent pembrolizumab as the

first-line treatment of *ROS1*+NSCLC given the overall survival benefit of Keynote-024 results for PD-L1 expression ($\geq 50\%$) and the FDA expanded approval of pembrolizumab approval of pembrolizumab for PD-L1 $\geq 1\%$ based on the Keynote-042 results as only *EGFR*+ and *ALK*+NSCLC were excluded and *ROS1*+NSCLC were not excluded from these studies [29, 30].

However, single agent immune checkpoint inhibitor appears to have limited activity in actionable driver mutation positive NSCLC. It is generally recognized that single agent immunotherapy is not effective in *EGFR* mutated NSCLC [31, 32]. Although evidence in *ROS1* fusion positive NSCLC is limited, a global registry has shown limited ORR of immune checkpoint inhibitors in NSCLC harboring oncogenic alterations with reported ORR of *ROS1* fusion+patients being 17% ($n=7$) and 12% ($n=125$) for *EGFR* mutated patients [33]. While better than the ORR of 12% in *EGFR* mutated patients, immunotherapy as a single agent may not be as effective as other options in *ROS1* fusion+NSCLC. Although statistically non-significant and limited analysis due to small sample size, our study also showed that the time on treatment was less with immunotherapy versus *ROS1* targeted TKIs in *ROS1*+NSCLC. Further prospective data on efficacy as well as safety are warranted.

Overall the incidence of *ROS1*+NSCLC detected in this database was lower than the generally accepted approximately 2% incidence in the literature [16]. Targeted RNA NGS and WTS are the most vigorous platforms in detecting RTK fusions where the transcribed RNA are detected and the reading frame is checked to ensure it is "in frame". In this study, there was no difference in the detection rates of *ROS1*+ by ArcherDx fusion assay (0.52%, 55/9393 and WTS (0.55%, 155/28173) in the NSCLC cohort which constituted the majority of the *ROS1* fusions.

One of the limitations of this study is the fact that there may be selection bias in those who were offered molecular testing. This is likely due to selection biases as *ROS1* fusions may be detected first by FISH and DNA NGS and RNA NGS are likely being employed when the tumor are "pan-negative". Additionally, there may have been further selection bias based on the baseline characteristics of patients such as smoking status, age, gender, and histology (i.e. in NSCLC, adenocarcinoma may likely be offered NGS more frequently than other histologies). Another limitation of this study is the lack of detailed clinical information regarding the timing of when the molecular analysis was performed (i.e. stage, pre vs post treatment evaluation). Outcomes were inferred based on time from tissue collection to date of last contact or time on treatment. In reality, NGS is performed at varying time points during the course of the disease and treatments.

Conclusions

Despite limitations, we were able to determine the characteristics of *ROS1* fusions in a tumor agnostic manner. *ROS1* fusions were identified in multiple tumor types. Only 78.8% with NSCLC have approved *ROS1* targeted therapy. Further studies to investigate the role of tyrosine kinase inhibitors in the approximately one fifth of solid tumors with *ROS1* fusions would be warranted. Finally, a more detailed examination of the clinical effects of other co-existing mutations along with underlying biological and molecular mechanism including high PDL1 score and having concurrent alterations such as *TP53* to account for the differences in survival outcomes of various *ROS1* fusions is eagerly awaited.

Abbreviations

ALK	Anaplastic lymphoma kinase
ATP	Adenosine triphosphate
CI	Confidence interval
CLIA	Clinical laboratory improvement amendments
CNS	Central nervous system
DNA	Deoxyribonucleic acid
FDA	Food and Drug Administration
FFPE	Formalin-fixed paraffin embedded
FGFR	Fibroblastic growth factor receptor
FISH	Fluorescence in situ hybridization
EGFR	Epidermal growth factor receptor
GBM	Glioblastoma multiforme
IMT	Inflammatory myofibroblastic tumor
IRB	Institutional review board
MB	Megabase
NGS	Next generation sequencing
NSCLC	Non-small cell lung cancer
NTRK	Neurotrophin receptor tyrosine kinase
PCR	Polymerase chain reaction
PD-L1	Programmed cell death ligand 1
RET	Rearranged in transformation
RNA	Ribonucleic acid
RTK	Receptor tyrosine kinase
ROS1	C-ROS1
TKI	Tyrosine kinase inhibitor
TMB	Tumor mutation burden
TPS	Tumor proportion score
WTS	Whole transcriptome sequencing

Supplementary Information

The online version contains supplementary material available at <https://doi.org/10.1186/s12885-023-11457-2>.

Additional file 1: Supplementary Figure 1. TPS score and TMB in ROS1+ NSCLC cohort.

Additional file 2: Supplementary Table 1. ROS1 fusions among solid tumors. **Supplementary Table 2.** Fusion partners and ROS1 exons.

Supplementary Table 3. Mean Junction read among tumor types.

Supplementary Table 4. Co-occurring alterations in ROS1+ NSCLC.

Supplementary Table 5. Distribution of PDL1 TPS score among ROS1+ NSCLC. **Supplementary Table 6.** Distribution of PDL1 TPS score among ROS1+ tumors.

Acknowledgements

Not applicable.

Authors' contributions

Misako Nagasaka, MD: Conceptualization; Data curation; Formal analysis; Investigation; Methodology; Project administration; Validation; Visualization; Roles/Writing – original draft and Writing – review & editing. Shannon S. Zhang, MD: Data curation; Formal analysis; Methodology; Roles/Writing – original draft and Writing – review & editing. Yasmine Baca, PhD: Data curation; Formal analysis; Investigation; Methodology and Roles/Writing – review & editing. Joanne Xiu, PhD: Data curation; Formal analysis; Investigation; Methodology and Roles/Writing – review & editing. Jorge Nieva, MD: Formal analysis; Investigation; Methodology and Roles/Writing – review & editing. Ari Vanderwalde, MD, MPH: Formal analysis; Investigation; Methodology and Roles/Writing – review & editing. Jeffrey J. Swensen, PhD: Formal analysis; Investigation; Methodology and Roles/Writing – review & editing. David Spetzler, MS, PhD, MBA: Formal analysis; Investigation; Methodology and Roles/Writing – review & editing. Wolfgang Michael Korn, MD, PhD: Formal analysis; Investigation; Methodology and Roles/Writing – review & editing. Luis E. Raez, MD: Formal analysis; Investigation; Methodology and Roles/Writing – review & editing. Stephen V. Liu, MD: Formal analysis; Investigation; Methodology and Roles/Writing – review & editing. Sai-Hong Ignatius Ou, MD PhD: Conceptualization; Formal analysis; Investigation; Methodology; Project administration; Resources; Software; Supervision; Validation; Visualization and Roles/Writing review & editing.

Funding

This study did not receive any funding.

Availability of data and materials

All data generated or analysed during this study are included in this manuscript and its supplementary files. The datasets generated during and/or analyzed during the current study are available from the corresponding author on reasonable request. The deidentified sequencing data are owned by Caris Life Sciences, and cannot be publicly shared due to the data usage agreement signed by Dr. Sai-Hong Ignatius Ou. Qualified researchers can apply for access to these summarized data by contacting Joanne Xiu, PhD (jxiu@caris.com) and signing a data usage agreement. The authors will honor legitimate requests for data sharing to qualified researchers, upon request, as necessary for conducting a methodologically sound research.

Declarations

Ethics approval and consent to participate

This study was conducted in accordance with guidelines of the Declaration of Helsinki, Belmont report, and U.S. Common rule. In keeping with 45 CFR 46.101(b)(4), this study was performed utilizing retrospective, deidentified clinical data. Therefore this study is considered IRB exempt and no patient consent was necessary from the subject. The need for written informed consent and ethical approval was waived by the University of California Irvine ethic committee due to the retrospective nature of the study.

Consent for publication

Not applicable as no individual identifying image or information are included in the manuscript.

Competing interests

There was no funding allocated for this research and there are no direct conflicts of interest. Potential COI from all authors are listed below.

Conflict of interest statement

MN is on the advisory board for AstraZeneca, Daiichi Sankyo, Takeda, Novartis, EMD Serono, Janssen, Pfizer, Eli Lilly and Company and Genentech; consultant for Caris Life Sciences (virtual tumor board); speaker for Blueprint Medicines and Takeda; and reports travel support from AnHeart Therapeutics.

SSZ has no disclosures.

YB, JX, JS, DS are employees and shareholders of Caris Life Sciences.

JN discloses the following: Consulting: Aadi Biosciences, Astra Zeneca, Bristol Myers Squibb, Fujirebio, G1 Therapeutics, Genentech, Mindmed, Naveris, Takeda, Western Oncolytics., Research Support: Genentech, Merck, Intellectual Property: Cansera and Ownership Interests: Cansera, Epic Sciences, Indee Bio, Quantgene.

AV is an employee of Caris Life Sciences and a consultant for West Cancer Center and George Clinical.

WMK has stock ownership of Caris Life Sciences.

LER has received research support from BMS, Astra-Zeneca, Roche, Pfizer, Merck, Velos, Guardant Health, Natera, Genentech, Bio Alta. SVL has received advisory fees from AstraZeneca, Blueprint, Bristol-Myers Squibb, Celgene, G1 Therapeutics, Genentech/Roche, Guardant Health, Inivata, Janssen, Jazz, Lilly, Merck/MSD, PharmaMar, Pfizer, Regeneron and Takeda; non-financial support from AstraZeneca, Boehringer-Ingelheim, Genentech/Roche, and Merck/MSD; and research grant support (to institution) from Alkermes, AstraZeneca, Bayer, Blueprint, Bristol-Myers Squibb, Corvus, Genentech, Janssen, Lilly, Lycera, Merck, Molecular Partners, Pfizer, Rain Therapeutics, RAPT, Spectrum, and Turning Point Therapeutics. SHIO has stock ownership and was on the scientific advisory board of Turning Point Therapeutics Inc (until Feb 28, 2019), is a member of the SAB of Elevation Oncology, and has received speaker honorarium from Merck, Roche/Genentech, Astra Zeneca, Takeda/ARIAD and Pfizer; has received advisory fees from Roche/Genentech, Astra Zeneca, Takeda/ARIAD, Pfizer, Foundation Medicine Inc, Spectrum, Daiichi Sankyo, Jassen/JNJ, and X-Covery.

Author details

¹Department of Medicine, Division of Hematology and Oncology, University of California Irvine School of Medicine, 200 South Manchester Ave, Orange, CA 92868, USA. ²Chao Family Comprehensive Cancer Center, Orange, CA, USA. ³Department of Internal Medicine, Division of Neurology, St. Marianna University School of Medicine, Kawasaki, Kanagawa, Japan. ⁴Caris Life Sciences, Phoenix, AZ, USA. ⁵USC Norris Comprehensive Cancer Center, University of Southern California Keck School of Medicine, Los Angeles, CA, USA. ⁶University of California San Francisco, San Francisco, CA, USA. ⁷Memorial Healthcare System/Florida Atlantic University, Pembroke Pines, FL, USA. ⁸Georgetown Lombardi Comprehensive Cancer Center, Georgetown University School of Medicine, Washington, DC, USA.

Received: 27 March 2023 Accepted: 28 September 2023

Published online: 18 October 2023

References

- Schram AM, Chang MT, Jonsson P, et al. Fusions in solid tumours: diagnostic strategies, targeted therapy, and acquired resistance. *Nat Rev Clin Oncol*. 2017;14:735–48.
- Blume-Jensen P, Hunter T. Oncogenic kinase signalling. *Nature*. 2001;411:355–65.
- Philip PA, Azar I, Xiu J, et al. Molecular Characterization of KRAS Wild-type Tumors in Patients with Pancreatic Adenocarcinoma. *Clin Cancer Res*. 2022;28(12):2704–14.
- Marabelle A, Fakih M, Lopez J, et al. Association of tumour mutational burden with outcomes in patients with advanced solid tumours treated with pembrolizumab: prospective biomarker analysis of the multicohort, open-label, phase 2 KEYNOTE-158 study. *Lancet Oncol*. 2020;10:1353–65.
- Merino DM, McShane LM, Fabrizio D, et al. Establishing guidelines to harmonize tumour mutational burden (TMB): in silico assessment of variation in TMB quantification across diagnostic platforms: phase I of the Friends of Cancer Research TMB Harmonization Project. *J Immunother Cancer*. 2020;8(1):e000147.
- Li W, Liu Y, Li W, et al. Intergenic breakpoints identified by DNA sequencing confound targetable kinase fusion detection in NSCLC. *J Thorac Oncol*. 2020;15(7):1223–31.
- Li W, Guo L, Liu Y, et al. Potential unreliability of uncommon ALK, ROS1, and RET genomic breakpoints in predicting the efficacy of targeted therapy in NSCLC. *J Thorac Oncol*. 2020;15(56-0864(20)):31023–6.
- Shaw AT, Ou SH, Bang YJ, et al. Crizotinib in ROS1-rearranged non-small-cell lung cancer. *N Engl J Med*. 2014;371:1963–71.
- Drilon A, Siena S, Dziadziuszko R, et al. Entrectinib in ROS1 fusion-positive non-small-cell lung cancer: integrated analysis of three phase 1–2 trials. *Lancet Oncol*. 2020;21:261–70.
- Birchmeier C, Sharma S, Wigler M. Expression and rearrangement of the ROS1 gene in human glioblastoma cells. *Proc Natl Acad Sci U S A*. 1987;84(24):9270–4.
- Yun MR, Kim DH, Kim SY, et al. Repotrectinib exhibits potent antitumor activity in treatment-naïve and solvent-front-mutant ROS1-rearranged non-small cell lung cancer. *Clin Cancer Res*. 2020;26(13):3287–95.
- Ou S-H, Fujiwara Y, Shaw AT, et al. Efficacy of Taletrectinib (AB-106/DS-6051b) in ROS1+ NSCLC: An Updated Pooled Analysis of U.S. and Japan Phase 1 Studies. *JTO Clinical and Research Reports*. 2(1) (2021). Available from: [https://www.jtocrr.org/article/S2666-3643\(20\)30154-5/fulltext](https://www.jtocrr.org/article/S2666-3643(20)30154-5/fulltext).
- Pelish HE, Tangpeerachaikul A, Kohl NE, Porter JR, Shair MD, Horan JC. NUV-520 (NVL-520) is a brain-penetrant and highly selective ROS1 inhibitor with antitumor activity against the G2032R solvent front mutation. *Cancer Res*. 2021. 81(13_Supplement):1465. https://aacrjournals.org/cancerres/article/81/13_Supplement/1465/667340/Abstract-1465-NUV-520-NVL-520-is-a-brain-penetrant.
- Turner J, Coutts K, Sheren J, Saichaemchan S, Ariyawutyakorn W, Avolio I, et al. Kinase gene fusions in defined subsets of melanoma. *Pigment Cell Melanoma Res*. 2017;30(1):53–62.
- Lovly CM, Gupta A, Lipson D, Otto G, Brennan T, Chung CT, et al. Inflammatory myofibroblastic tumors harbor multiple potentially actionable kinase fusions. *Cancer Discov*. 2014;4:889–95.
- Zhu Q, Zhan P, Zhang X, et al. Clinicopathologic characteristics of patients with ROS1 fusion gene in non-small cell lung cancer: a meta-analysis. *Transl Lung Cancer Res*. 2015;4(3):300–9.
- Hu H, Ding N, Zhou H, Wang S, Tang L, Xiao Z. A novel CD74-ROS1 gene fusion in a patient with inflammatory breast cancer: a case report. *J Med Case Rep*. 2021;15(1):277.
- Tao Z, Liu J, Li T, Xu H, Chen K, Zhang J, et al. Profiling receptor tyrosine kinase fusions in Chinese breast cancers. *Front Oncol*. 2021;11:741142.
- Pishvaian MJ, Garrido-Laguna I, Liu SV, Multani PS, Chow-Maneval E, Rolfo C. Entrectinib in TRK and ROS1 fusion-positive metastatic pancreatic cancer. *JCO Precis Oncol*. 2018;2:1–7.
- Gu TL, Deng X, Huang F, Tucker M, Crosby K, Rimkunas V, et al. Survey of tyrosine kinase signaling reveals ROS kinase fusions in human cholangiocarcinoma. *PLoS ONE*. 2011;6:e15640.
- Lee J, Lee SE, Kang SY, Do IG, Lee S, Ha SY, et al. Identification of ROS1 rearrangement in gastric adenocarcinoma. *Cancer*. 2013;119:1627–35.
- Donati M, Kastnerova L, Martinek P, et al. Spitz tumors with ROS1 fusions: A clinicopathological study of 6 cases, including FISH for chromosomal copy number alterations and mutation analysis using next-generation sequencing. *Am J Dermatopathol*. 2020;42(2):92–102.
- Pietrantonio F, Di Nicolantonio F, Schrock AB, Lee J, Tejpar S, Sartore-Bianchi A, et al. ALK, ROS1, and NTRK rearrangements in metastatic colorectal cancer. *J Natl Cancer Inst*. 2017;109(12).
- Ritterhouse LL, Wirth LJ, Randolph GW, Sadow PM, Ross DS, Liddy W, et al. ROS1 rearrangement in thyroid cancer. *Thyroid*. 2016;26:794–7.
- Ou SI, Nagasaka M. Catalog of 5' fusion partners of ROS1+ NSCLC circa 2020. *JTO Clin Res Rep*. 2020;1(3):100048.
- Neel DS, Allegakoen DV, Olivas V, et al. Differential subcellular localization regulates oncogenic signaling by ROS1 kinase fusion proteins. *Cancer Res*. 2019;79(3):546–56.
- Li Z, Shen L, Ding D, et al. Efficacy of crizotinib among different types of ROS1 fusion partners in patients with ROS1-rearranged non-small cell lung cancer. *J Thorac Oncol*. 2018;13:987–95.
- Kron A, Alidousty C, Scheffler M, et al. Impact of TP53 mutation status on systemic treatment outcome in ALK-rearranged non-small-cell lung cancer. *Ann Oncol*. 2018;29:2068–75.
- Reck M, Rodríguez-Abreu D, Robinson AG, et al. Updated analysis of KEYNOTE-024: Pembrolizumab versus platinum-based chemotherapy for advanced non-small-cell lung cancer with PD-L1 tumor proportion score of 50% or greater. *J Clin Oncol*. 2019;37:537–46.
- Mok TSK, Wu YL, Kudaba I, et al. Pembrolizumab versus chemotherapy for previously untreated, PD-L1-expressing, locally advanced or metastatic non-small-cell lung cancer (KEYNOTE-042): a randomised, open-label, controlled, phase 3 trial. *Lancet*. 2019;393:1819–30.
- Lisberg A, Cummings A, Goldman JW, et al. A phase II study of Pembrolizumab in EGFR-Mutant, PD-L1+, Tyrosine Kinase inhibitor naïve patients with advanced NSCLC. *J Thorac Oncol*. 2018;13(8):1138–45.
- Gainor JF, Shaw AT, Sequist LV, et al. EGFR Mutations and ALK rearrangements are associated with low response rates to PD-1 pathway blockade in non-small cell lung cancer: a retrospective analysis. *Clin Cancer Res*. 2016;22(18):4585–93.
- Mazieres J, Drilon A, Lusque A, et al. Immune checkpoint inhibitors for patients with advanced lung cancer and oncogenic driver alterations: results from the Immunotarget registry. *Ann Oncol*. 2019;30:1321–8.

Publisher's Note

Springer Nature remains neutral with regard to jurisdictional claims in published maps and institutional affiliations.